

# ATP Synthase: Two rotary molecular motors working together

George Oster  
Hongyun Wang

University of California, Berkeley

## Introduction

ATP synthase—also called  $F_0F_1$  ATPase, or simply F-ATPase—is the universal protein that terminates oxidative phosphorylation by synthesizing ATP from ADP and phosphate. Nearly identical proteins are found in eukaryotic mitochondria and bacteria, and they all operate on the same principle. Electron driven ion pumps set up concentration and electrical gradients across a membrane. ATP synthase utilizes the energy stored in this electrochemical gradient to drive nucleotide synthesis. It does this in a surprising way: by converting the electromotive force into a rotary torque that is used to promote phosphate binding and to liberate ATP from the catalytic site where it was formed. Remarkably, this process can be reversed in certain circumstances: ATP hydrolysis can drive the engine in reverse so that F-ATPase functions as a proton pump. Indeed, the vacuolar V-ATPases—the most ubiquitous intracellular proton pumps—are structurally similar to ATP synthase and appear to operate according to the same principles.

ATP synthase is composed of at least 8 subunit types, whose stoichiometry is denoted with subscripts:  $(\alpha_3, \beta_3, \gamma, \delta, \epsilon, a_6, b_2, c_{12})$ , which combine into two distinct regions. The geometric arrangement of the subunits is shown schematically in **Figure 1a**. The  $F_1$  portion is soluble and consists of a hexamer,  $\alpha_3\beta_3$ . This hexamer is arranged in an annulus about a central shaft consisting of the coiled-coil  $\gamma$  subunit. Subunits  $\delta$  and  $\epsilon$  generally isolate with  $F_1$  as well. The  $F_0$  portion consists of three transmembrane subunits:  $a_6$ ,  $b_2$  and  $c_{12}$ . 12 copies of the c-subunit form a disk into which the  $\gamma$  and  $\epsilon$  subunits insert. The remainder of  $F_0$  consists of the transmembrane subunits  $a_6$  and  $b_2$ ;

the latter is attached by the  $\delta$  subunit to an  $\alpha$  subunit so that it anchors the a subunit to  $F_1$ . Thus there are two 'stalks' connecting  $F_0$  to  $F_1$ :  $\gamma\epsilon$  and  $b_2\delta$ .

The key to understanding how ATP synthase carries out its catalytic and synthetic roles lies in this geometric organization. The entire protein can be divided into two *operational* regions denoted suggestively as the 'rotor' and 'stator' for reasons that derive from the rotary mechanism by which the protein operates (**Figure 1b**). Indeed, it turns out that ATP synthase is two rotary engines in one. The  $F_0$  motor converts transmembrane electrochemical energy into a rotary torque on the  $\gamma$  shaft, and  $F_1$  uses ATP hydrolysis to turn the  $\gamma$  shaft in the opposite direction. Since they are connected, one drives the other in reverse: when  $F_0$  dominates, the rotor turns clockwise (looking upwards in **Figure 1**) so that  $F_1$  synthesizes ATP. When  $F_1$  dominates, so that  $F_0$  is driven counterclockwise, it can pump protons against an electrochemical gradient. Deciphering how this remarkable dual energy transduction works is one of the great triumphs of modern chemistry.

**Figure 1.** (a) Schematic diagram of the subunit organization of ATP synthase showing the  $\alpha_3\beta_3$  hexamer and a portion of the  $\gamma$  shaft. The lower part of  $\gamma$  has not been resolved. The c-subunit consists of 12 pairs of transmembrane  $\alpha$ -helices, and the a subunit of 6 transmembrane  $\alpha$ -helices. The  $\epsilon$  subunit abuts c and  $\gamma$ , and interacts with the DELSEED region of  $\beta$ . The a subunit is attached to an  $\alpha$  subunit via the b and  $\delta$  subunits. (b) Torque is generated by the protonmotive force at the a-c interface, leading to the functional subdivision into two counter-rotating assemblies, usually denoted as the 'rotor' and 'stator'. The rotor consists of subunits  $c_{12}\text{-}\gamma\text{-}\epsilon$ , and the stator consists of subunits  $a\text{-}b_2\text{-}\delta\text{-}\alpha_3\beta_3$ .

## ATP synthesis in $F_1$ is driven by the rotation of the $\gamma$ -shaft

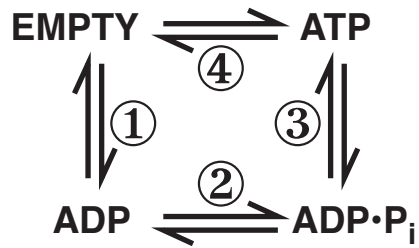
We begin with the  $F_1$  motor because we now know precisely what it looks like. This is due to John Walker and his x-ray crystallography group at Cambridge, who worked out the exact structure of the  $\alpha_3\beta_3$  hexamer and most of the  $\gamma$  shaft (1). A stereo view of the structure is shown in **Figure 2**. Walker was awarded the Nobel Prize in 1997, for his structure revealed essential asymmetries in the molecule's structure that were the key

to understanding how it worked. In the early 1980's, Paul Boyer at UCLA, proposed the surprising theory that, in the catalytic sites of  $F_1$ , ATP was in chemical equilibrium with its reactants, ADP and phosphate (2). So the formation of ATP was essentially energetically without cost. However, since each ATP when hydrolyzed under cellular conditions liberates about 12 kcal/mol, this energetic price must be paid at some point. Boyer proposed that  $F_1$  pays this price in the mechanical work necessary to liberate the nucleotide from the catalytic site. Further, release of product (ATP) proceeds sequentially and cyclically around the  $\alpha_3\beta_3$  hexamer because the synthetic reactions are synchronized in a fixed phase relation by the rotation of the  $\gamma$  shaft and cooperative coupling between the three catalytic sites. Boyer's 'binding change' mechanism neatly fits the Walker structure, and Boyer shared with Walker the 1997 Nobel Prize. A schematic diagram of the binding change mechanism is shown in **Figure 3**.

**Figure 2.** Stereo pair showing the molecular structure of the  $F_1$  subunit. The  $\alpha$  subunit is in yellow, the two coils of the  $\gamma$  subunit are blue and gray, and its asymmetric structure is evident. The  $\beta$  subunit is in two colors: the stationary upper barrel segment is in green, and the lower hinge segment is red. The structure of the  $\epsilon$  subunit (not shown) is known, but how it attaches to the  $\gamma$  and  $c$  subunits is not clear.

**Figure 3.** The binding change mechanism. Notation for site occupancies: T = ATP bound, DP = ADP• $P_i$  bound, D = ADP bound.  $\beta$  subunits are numbered clockwise. The length of the arrows indicates the relative binding affinities (a) The system starts with either  $(\beta_1, \beta_2, \beta_3) = (E, T \rightleftharpoons D \bullet P, D)$  or  $(\beta_1, \beta_2, \beta_3) = (D, T \rightleftharpoons D \bullet P, D)$ . (b) Clockwise rotation of  $\gamma$  increases the binding affinity of ADP in  $\beta_1$ , traps ATP in  $\beta_2$ , and promotes  $P_i$  binding on  $\beta_3$ . (c) Further rotation of  $\gamma$  traps ADP and allows  $P_i$  binding in  $\beta_1$ , releases the tightly bound ATP and allows ADP binding in  $\beta_2$ , and traps  $P_i$  in  $\beta_3$ .

There are actually 6 nucleotide binding sites on the  $\alpha_3\beta_3$  hexamer, all lying at the interfaces between the  $\alpha$  and  $\beta$  subunits. The catalytic sites lie mostly in the  $\beta$  subunit, while the noncatalytic sites lie mostly in the  $\alpha$  subunit. The role of the noncatalytic sites is uncertain, but may help hold the hexamer together. Each catalytic site traverses the synthetic cycle sequentially:



In steps 1 and 2 a site binds ADP and phosphate (not necessarily in that order). While trapped in the catalytic site in step 3, reactants (ADP and P<sub>i</sub>) and product (ATP) are in chemical equilibrium. Step 4 requires the input of mechanical torque from F<sub>o</sub> on  $\gamma$  to trap the reactants in the ATP state and to pry open the site releasing the tightly bound ATP. Most of the 12 kcal/mol price of synthesis is paid in step 4. The way in which this works is found in the shape of the  $\alpha_3\beta_3$  hexamer and the  $\gamma$  shaft.

The  $\gamma$  subunit is asymmetric and bowed. It fits into a central annulus in the  $\alpha_3\beta_3$  which is itself asymmetric (**Figure 4**). At the top of the  $\alpha_3\beta_3$  hexamer is a hydrophobic 'sleeve' in which the  $\gamma$  shaft rotates. Further down, however, the annulus is offset from the center, so that as  $\gamma$  rotates clockwise, it sequentially pushes outwards on each catalytic site. In addition, the  $\epsilon$  subunit is located eccentrically and attached to the  $\gamma$  and c subunits so that, as  $\gamma$  rotates, it comes into contact sequentially with each  $\beta$  subunit in a conserved region called the DELSEED sequence (named for the single letter abbreviation of its constituent amino acids). Together, this asymmetric rotation exerts stress on the catalytic site loosening its grip on ATP so that thermal fluctuations can free it into solution.

The catalytic sites do not act independently; rather they are synchronized so that each site traverses the synthetic cycle in a more or less fixed phase with respect to the others. This synchronization is orchestrated in several ways. As the  $\gamma$  shaft rotates, it not only stresses each catalytic site, but it also interacts electrostatically with the  $\beta$  subunits at two locations (3). These interactions may mediate phosphate and nucleotide binding, the necessary precursors to synthesis. In addition, the catalytic sites appear to be elastically coupled so that the occupancy of one site affects the affinity of the other two sites. The consequence of this coupling is that when ATP concentrations are low enough so that

only one site is occupied, hydrolysis proceeds much more slowly than when more than one site is occupied.

Together with the  $F_1$  molecular structure, the binding change model strongly supported the idea that catalysis involved rotation of the  $\gamma$  subunit. However, dramatic visual confirmation was provided by *in vitro* experiments in which the  $\alpha_3\beta_3\gamma$  subunits were isolated and attached to a bead. A fluorescently tagged actin filament was attached to the  $\gamma$  shaft and, when ATP was supplied, the filament could clearly be seen to rotate. In fact, a complete revolution took place in 3 steps, and consumed a single ATP per step (4).

The viscous drag on the actin filament could be estimated, which allowed the torque developed by the  $F_1$  motor to be computed and compared with the free energy available from ATP hydrolysis. The startling result was that the motor generated an average torque of more than 40 piconewton nanometers ( $40 \times 10^{-12} \text{ N} \times 10^{-9} \text{ m}$ ), more than six times the maximum force developed by kinesin or myosin. More impressively, the motor operated near 100% mechanical efficiency; this precludes any sort of heat engine that would be limited by the Carnot efficiency (4). Several models have been proposed that address the issue of torque generation and efficiency (4-6).

The energy to drive this motion derives from the hydrolysis cycle of ATP at the catalytic site. Moreover, the conformational change that drives the hydrolysis motor must be nearly the reverse of the motion that frees ATP from the catalytic site during synthesis. Examination of Walker's structure reveals that the major conformational change is a hinge-bending motion in  $\beta$  subunits. The bottom portion of each  $\beta$  below the nucleotide binding site rotates inward approximately  $30^\circ$  during which it pushes on the bowed  $\gamma$  subunit, turning it much like one cranks an automobile jack (**Figure 4**).

**Figure 4.** Cross section of  $F_1$  showing the conformational changes in the  $\beta$  subunits that drive rotation of  $\gamma$ . The  $\alpha$  subunit is in yellow and the stationary barrel region of  $\beta$  is in green. During the hydrolysis cycle, the lower segment of  $\beta$ , shown in red, undergoes a hinge-bending motion that rotates it about  $30^\circ$  inwards. This motion pushes on the eccentric  $\gamma$  coiled-coil causing it to rotate within the barrel bearing. During the synthesis, the rotation of  $\gamma$  pushes on each catalytic site. The panels show three snapshots of the motion during a  $180^\circ$  rotation. Movies of the rotational sequence can be downloaded from the authors' web site: [http://www.cnr.berkeley.edu/~goster/ATP\\_movies.html](http://www.cnr.berkeley.edu/~goster/ATP_movies.html).

## **$F_0$ converts protonmotive force into rotary torque**

There is currently no direct observations of rotation in the  $F_0$  portion of ATP synthase (7). However, current thinking is that the  $F_0$  assembly converts the energy contained in the transmembrane protonmotive force into a rotary torque at the interface of the a and c subunits (**Figure 1**). This torque turns the rotor (the c,  $\gamma$  and  $\epsilon$  subunits) which couples to the  $F_1$  synthetic machine.

The c assembly consists of 12 subunits, each consisting of two transmembrane  $\alpha$ -helices (8). There is one essential acidic amino acid (Asp61 in the *E. Coli* ATP synthase) which binds protons. Since there are variants of ATP synthase that can operate on sodium rather than protons, the interaction between the c subunit and the translocated ion has the property of an electrostatic carrier mechanism (9).

The a subunit consists of 6 transmembrane  $\alpha$ -helices which contain at least one essential basic residue (Arg210 in *E. Coli*) (8, 10). The interaction of these rotor and stator charges is essential for torque generation, and several proposals have been put forward for how this could work (11-14). Whatever the mechanism, the  $F_0$  motor must generate a torque sufficient to liberate 3 ATP's from the three catalytic sites in  $F_1$  for each revolution. If the proton flux through the stator is tightly coupled to the rotation of the c subunit, then a rotation of  $2\pi/3$  carries 4 protons down the electromotive potential of 230 mV typical of the mitochondrial inner membrane (14). This is sufficient to account for the mechanical energy required for synthesis of one ATP.

Under anaerobic conditions, the ATP synthase of the bacteria *E. Coli* can reverse its operation, hydrolyzing ATP and turning the c subunit backwards so that it functions as a proton pump. This is not surprising, since the F-ATPases are structurally similar to the most common proton pumps, the vacuolar, or V-ATPases (7). These pumps may have been the evolutionary precursors of ATP synthase (15). A striking difference between the two is that the F-ATPases have 12 acidic rotor charges, whereas the V-ATPases have 6. It can be shown that this enables the V-ATPases to function more efficiently as ion pumps, at the expense of relinquishing their capability to synthesize ATP.

## Summary

Both the  $F_1$  and  $F_o$  motors can operate in both directions.  $F_1$  is a hydrolysis-driven 3-piston engine which can be driven in reverse to synthesize ATP from ADP and phosphate.  $F_o$  is an ion-driven rotary engine which can be driven in reverse to function as an ion pump. The F-ATPases are structurally similar to, and presumably evolutionarily related to, the V-ATPase ion pumps (15). Most ion pumps are thought to function by an 'alternating access' mechanism whereby an ion is first bound strongly on the dilute side, then energy is supplied to move the ion such that it communicates with the concentrated side and to weaken its binding affinity (16). However, in contrast with other ion pumps, the F and V-ATPases accomplish this by a rotary mechanism that is driven indirectly by nucleotide hydrolysis, rather than by direct phosphorylation (17). The  $F_o$  motor is thought to be related also to the bacterial flagellar motor. Both can operate on sodium, although the flagellar motor has 8 or more 'stators' and develops far more torque than  $F_o$  (18) (19).

The mechanism driving the  $F_1$  hydrolysis motor may carry hints for other nucleotide hydrolysis fueled motors, such as kinesin, myosin and dynein. However, there are important structural differences that may make the comparison difficult (4). For example, the above mentioned motors all 'walk' along a polymer track to which they bind tightly during a portion of their mechanochemical cycle. The power stroke of the  $F_1$  motor is driven by the  $\beta$  subunit which pushes on the  $\gamma$  shaft, but does not appear to bind tightly to it; that is, it does not 'walk' around the  $\gamma$  shaft. Moreover, no other

motor operates with nearly the efficiency as the  $F_1$  motor, implying that there are important entropic steps in other motors that are absent in the  $F_1$  motor.



## Figure Captions

**Figure 1.** (a) Schematic diagram of the subunit organization of ATP synthase showing the  $\alpha_3\beta_3$  hexamer and a portion of the  $\gamma$  shaft. The lower part of  $\gamma$  has not been resolved. The c-subunit consists of 12 pairs of transmembrane  $\alpha$ -helices, and the a subunit of 6 transmembrane  $\alpha$ -helices. The  $\epsilon$  subunit abuts c and  $\gamma$ , and interacts with the DELSEED region of  $\beta$ . The a subunit is attached to an  $\alpha$  subunit via the b and  $\delta$  subunits. (b) Torque is generated by the protonmotive force at the a-c interface, leading to the functional subdivision into two counter-rotating assemblies, usually denoted as the 'rotor' and 'stator'. The rotor consists of subunits  $c_{12}$ - $\gamma$ - $\epsilon$ , and the stator consists of subunits a- $b_2$ - $\delta$ - $\alpha_3\beta_3$ .

**Figure 2.** Stereo pair showing the molecular structure of the  $F_1$  subunit. The  $\alpha$  subunit is in yellow, the two coils of the  $\gamma$  subunit are blue and gray, and its asymmetric structure is evident. The  $\beta$  subunit is in two colors: the stationary upper barrel segment is in green, and the lower hinge segment is red. The structure of the  $\epsilon$  subunit (not shown) is known, but how it attaches to the  $\gamma$  and c subunits is not clear.

**Figure 3.** The binding change mechanism. Notation for site occupancies: T = ATP bound, DP = ADP• $P_i$  bound, D = ADP bound.  $\beta$  subunits are numbered clockwise. The length of the arrows indicates the relative binding affinities (a) The system starts with either  $(\beta_1, \beta_2, \beta_3) = (E, T \leftrightarrow D \bullet P, D)$  or  $(\beta_1, \beta_2, \beta_3) = (D, T \leftrightarrow D \bullet P, D)$ . (b) Clockwise rotation of  $\gamma$  increases the binding affinity of ADP in  $\beta_1$ , traps ATP in  $\beta_2$ , and promotes  $P_i$  binding on  $\beta_3$ . (c) Further rotation of  $\gamma$  traps ADP and allows  $P_i$  binding in  $\beta_1$ , releases the tightly bound ATP and allows ADP binding in  $\beta_2$ , and traps  $P_i$  in  $\beta_3$ .

**Figure 4.** Cross section of  $F_1$  showing the conformational changes in the  $\beta$  subunits that drive rotation of  $\gamma$ . The  $\alpha$  subunit is in yellow and the stationary barrel region of  $\beta$  is in green. During the hydrolysis cycle, the lower segment of  $\beta$ , shown in red, undergoes a hinge-bending motion that rotates it about  $30^\circ$  inwards. This motion

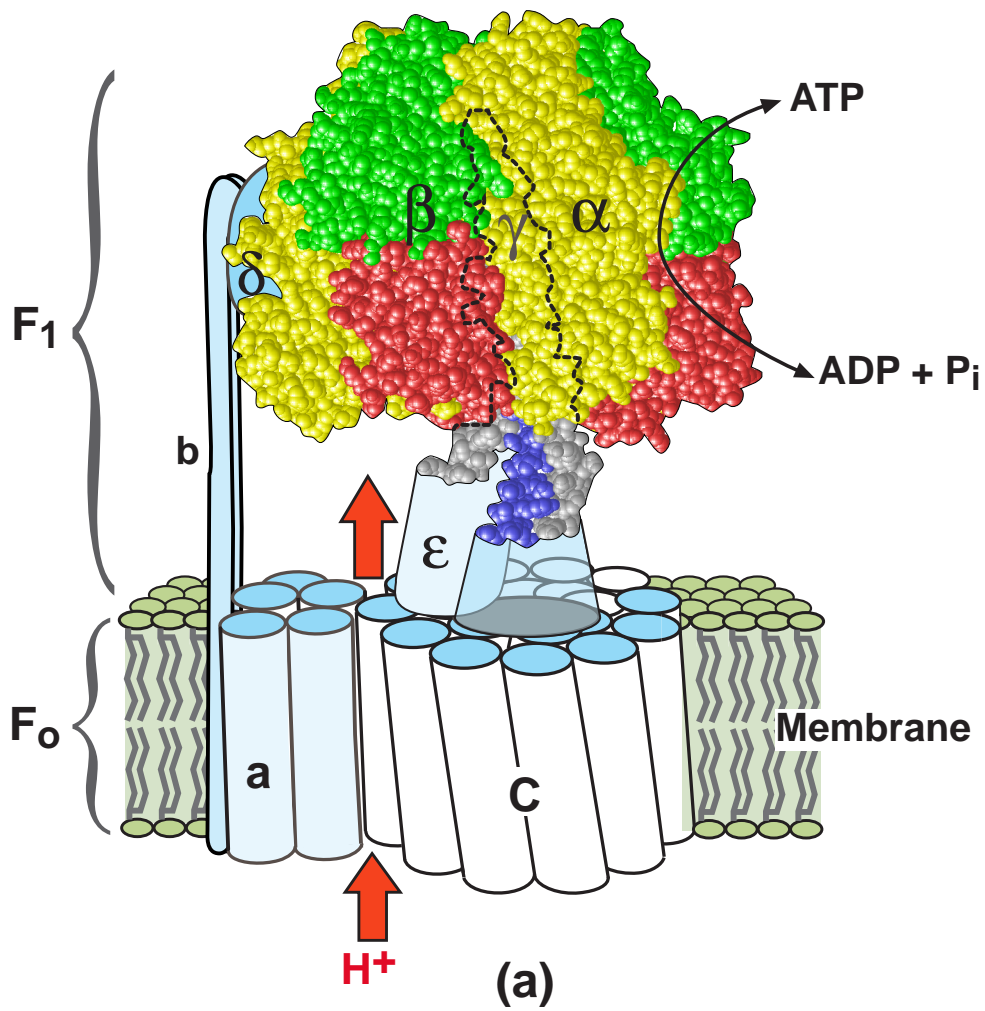
pushes on the eccentric  $\gamma$  coiled-coil causing it to rotate within the barrel bearing. During the synthesis, the rotation of  $\gamma$  pushes on each catalytic site. The panels show three snapshots of the motion during a  $180^\circ$  rotation. Movies of the rotational sequence can be downloaded from the authors' web site: [http://www.cnr.berkeley.edu/~goster/ATP\\_movies.html](http://www.cnr.berkeley.edu/~goster/ATP_movies.html).

## References

1. J. Abrahams, A. Leslie, R. Lutter and J. Walker (1994) *Nature* **370**, 621-628.
2. P. Boyer (1993) *Biochimica et Biophysica Acta* **1140**, 215-250.
3. M. Al-Shawi, C. Ketchum and R. Nakamoto (1997) *J. Biol. Chem.* **272**, 2300-2306.
4. K. Kinoshita, R. Yasuda, H. Noji, S. Ishiwata and M. Yoshida (1998) *Cell* **93**, 21-24.
5. F. Oosawa and S. Hayashi (1986) *Adv Biophys* **22**, 151-83.
6. H. Wang and G. Oster (1998) *Nature* **396**, 279-282.
7. M. Finbow and M. Harrison (1997) *Biochem. J.* **324**, 697-712.
8. R. H. Fillingame (1997) *J. Exp. Biol.* **200**, 217-224.
9. P. Dimroth (1997) *Biochimica et Biophysica Acta* **1318**, 11-51.
10. R. H. Fillingame (1996) *Current Opinion in Structural Biology* **6**, 491-8.
11. S. B. Vik and B. J. Antonio (1994) *J. Biol. Chem.* **269**, 30364-30369.
12. W. Junge, H. Lill and S. Engelbrecht (1997) *Trends Biochem. Sci.* **22**, 420-423.
13. G. Kaim, U. Matthey and P. Dimroth (1998) *EMBO J.* **17**, 688-695.
14. T. Elston, H. Wang and G. Oster (1998) *Nature* **391**, 510-514.
15. R. Cross and L. Taiz (1990) *FEBS Lett.* **259**, 227-229.
16. B. Alberts, D. Bray, J. Lewis, M. Raff, K. Roberts and J. Watson (1994) *Molecular Biology of the Cell* New York, Garland
17. S. Khan (1997) *Biochimica et Biophysica Acta* **1322**, 86-105.
18. H. Berg (1995) *Biophys. J.* **68**, 163s-166s.
19. K. Muramoto, I. Kawagishi, S. Kudo, Y. Magariyama, Y. Imae and M. Homma (1995) *J. Mol. Biol.* **251**, 50-58.

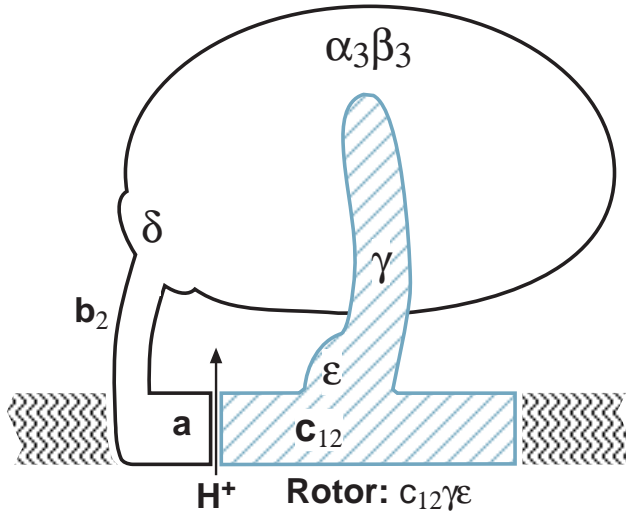
## Supplementary Reading

- Boyer, P. (1993). The binding change mechanism for ATP synthase--some probabilities and possibilities. *Biochimica et Biophysica Acta* **1140** : 215-250.
- Weber, J. and A. E. Senior (1997). Catalytic mechanism of F1-ATPase. *Biochim. Biophys. Acta* **1319** (1): 19-58.

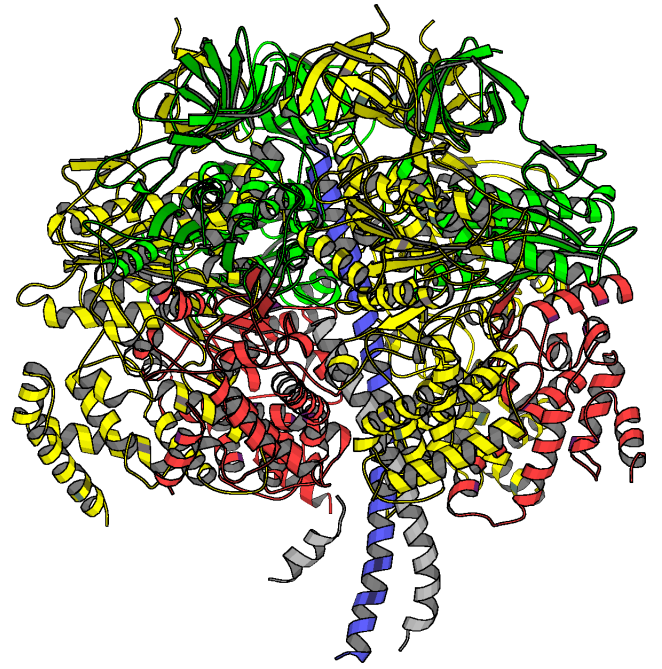


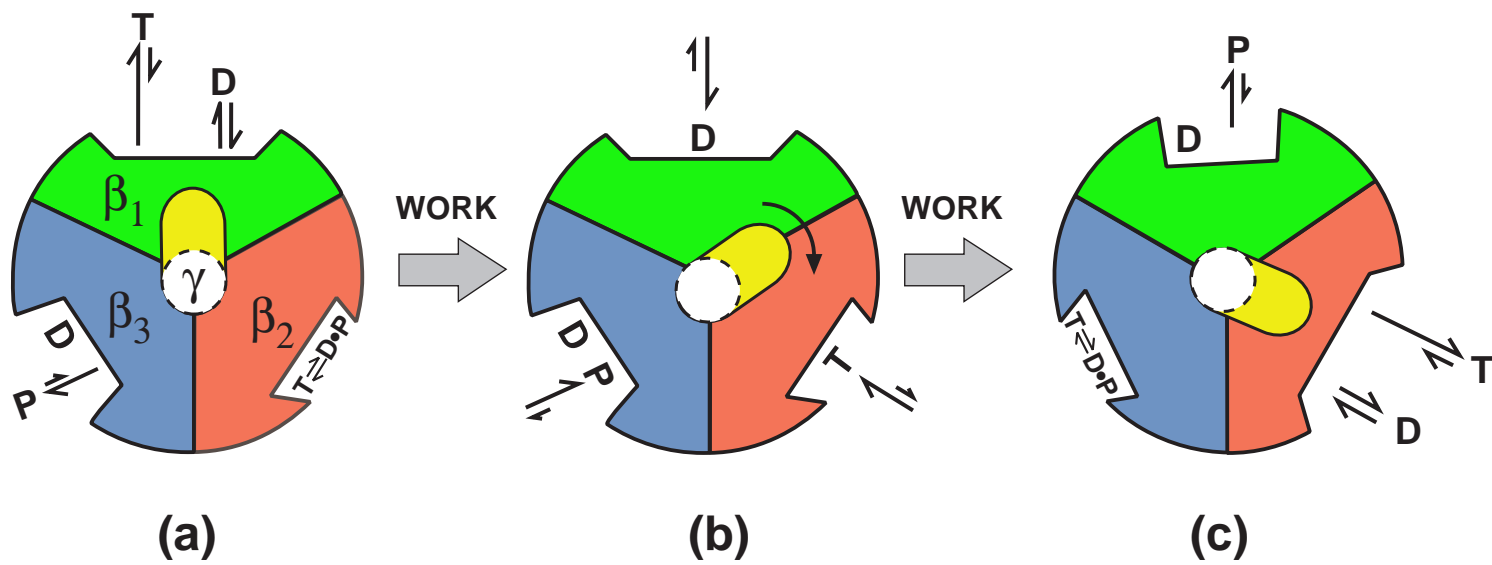
10 nm

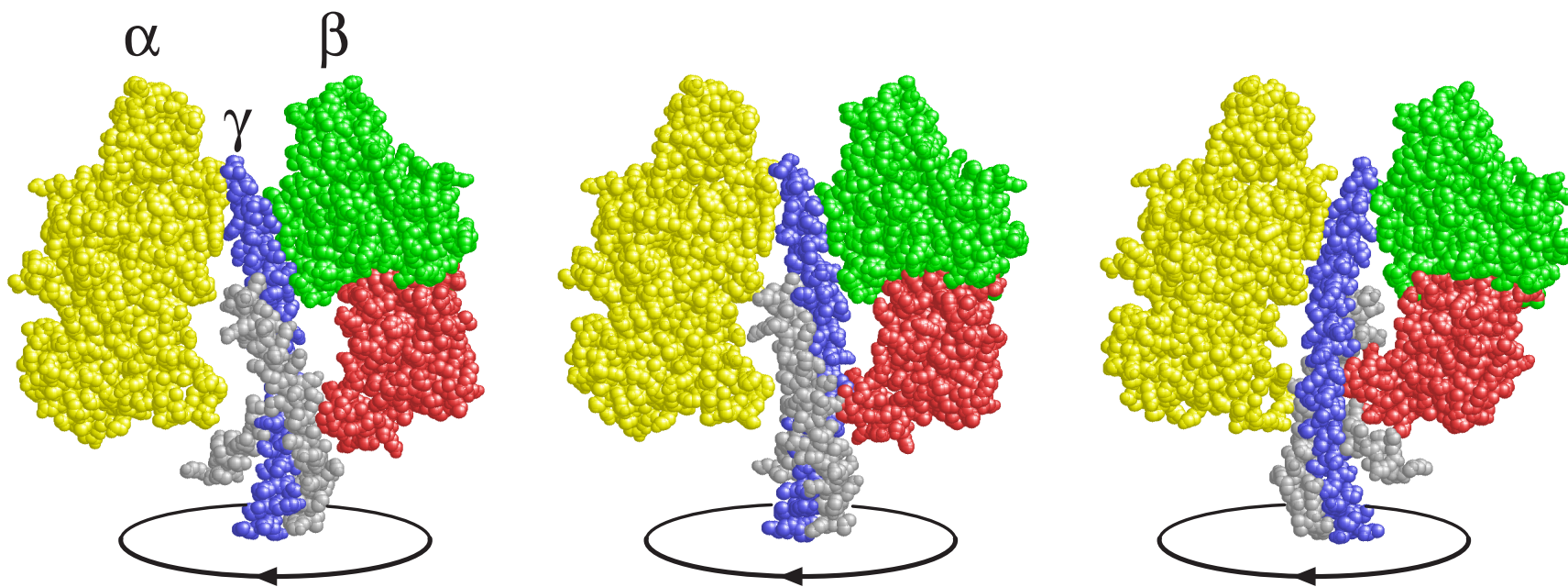
Stator:  $ab_2\delta\alpha_3\beta_3$



(b)







Oster & Wang  
Figure 4